Emerging nano-biosensing with suspended MNP microbial extraction and EANP labeling

Leann Lerie Matta, Evangelyn C. Alocilja

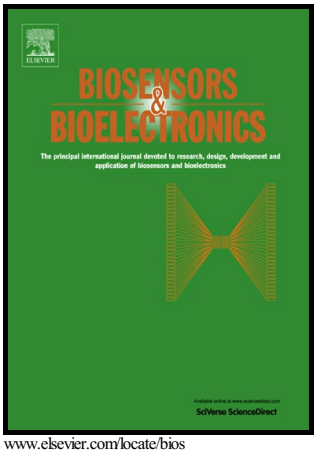

www.elsevier.com/locate/bios

PII: S0956-5663(18)30508-6
DOI: https://doi.org/10.1016/j.bios.2018.07.007
Reference: BIOS10596

To appear in: *Biosensors and Bioelectronic*

Received date: 17 April 2018
Revised date: 2 July 2018
Accepted date: 5 July 2018

Cite this article as: Leann Lerie Matta and Evangelyn C. Alocilja, Emerging nano-biosensing with suspended MNP microbial extraction and EANP labeling, *Biosensors and Bioelectronic,* https://doi.org/10.1016/j.bios.2018.07.007

Emerging nano-biosensing with suspended MNP microbial extraction and EANP labeling

Leann Lerie Matta and Evangelyn C. Alocilja*

Nano-Biosensors Lab, Biosystems and Agricultural Engineering, Michigan State University, East Lansing, MI 48824

*Corresponding author: Tel.: (517)-432-8672; Email: alocilja@msu.edu

Abstract

In ensuring a secure microbe-free food supply, rapid response detection of microbial contamination is of utmost importance. Many biosensor designs have been proposed over the past two decades, covering a broad range of binding ligands, signal amplification, and detection mechanisms. These designs may consist of self-contained test strips developed from the base up with complicated nanoparticle chemistry and intricate ligand immobilization. Other methods use multiple step-wise additions, many based upon ELISA 96-well plate technology with fluorescent detection. In addition, many biosensors use expensive antibody receptors or DNA ligands. But many of these proposed designs are impracticable for most applications or users, since they don't FIRST address the broad goals of any biosensor: Field operability, Inexpensive, with Real-time detection that is both Sensitive and Specific to target, while being as Trouble-free as possible. Described in this review are applications that utilize versatile magnetic nanoparticles (MNP) extraction, electrically active nanoparticles (EANP) labeling, and carbohydrate-based ligand chemistry. MNP provide rapid pathogen extraction from liquid samples. EANP labeling improves signal amplification and expands signaling options to include optical and electrical detection. Carbohydrate ligands are inexpensive, robust structures that are increasingly synthesized for higher selectivity. Used in conjunction with optical or electrical detection of gold nanoparticles (AuNP), carbohydrate-functionalized MNP-cell-AuNP nano-biosensing advances the goal of being the FIRST biosensor of choice in detecting microbial pathogens throughout our food supply chain.

Keywords: Nano-biosensors; Magnetic nanoparticles; Food supply chain security; Rapid detection; User-friendly; Gold nanoparticles; Microbial contamination; Carbohydrate-functionalized MNP-cell-AuNP biosensing

1. Introduction

Worldwide population growth is estimated to reach 9.8 billion people by 2050 (Adegoke, 2017). This growth will further task our food and water supplies. Currently over 28 billion meals are consumed each day around the globe (Beach, 2016). But foodborne disease sickened 600 million people in 2010, causing over 420,000 deaths from foodborne hazards, including those that were bacterial in origin. Unfortunately, children under the age of 5 years represented 40% of these illnesses (WHO, 2015). Higher mortality rates persistently hit under/developing countries in African sub-regions, South-East Asia and the Eastern Mediterranean (Havelaar et al., 2015; WHO, 2015), which have limited economical resources to fight these diseases.

Environmental microbial pathogens are a major concern, creating a double-edged sword for developing countries. Food and water scarcity create conditions in which contamination is ignored by starving people who can also ill afford to contract diseases. Even in the US, the majority of food outbreaks were caused by three pathogenic bacteria: *Salmonella*, Shiga Toxin producing *E. coli* and *Listeria monocytogenes* (Dewey-Mattia et al., 2014; FDA, 2015).Many biosensing assays, though, are too expensive or technically complicated to be economically feasible in many regions of the world. Economical methods should require minimal storage and technology, with long shelf life, , such as those developed in our Nano-Biosensors lab using carbohydrate-functionalized MNP and dextrin-coated gold nanoparticles (AuNP).

Sensor component miniaturization has led to nano-sized microbial biosensors (Fernandes et al., 2015; Gayathri et al., 2016; Liu et al., 2014; Setterington and Alocilja, 2012; Vetrone et al., 2012; Yazgan et al., 2014). Nano-biosensors are now prevalent within medical, environmental and even personal-use areas (Cheng et al., 2011; Kimura et al., 2009; Webster et al., 2015). Their cost is of little concern to the industrial user; but in under-developed countries, cost is the least concern. Many nano-biosensors designed to date also require expensive test equipment, environmentally sensitive components, refrigeration, and advanced training (Chen et al., 2015; Malic et al., 2015). A truly successful biosensor design incorporates high sensitivity with fast responses that are easily deciphered and require little manual labor and supplies.

Current nano-biosensing methods show specificity that ranges from non-selective bacterial attachment to surfaces, to selective capture using monoclonal antibodies or DNA-aptamer binding. Detection methods vary from “visual” reporting of aggregated nanoparticles, to electrical and electrochemical signaling. Magnetic nanoparticles (MNP) are beneficial in all of these applications due to their large surface area to volume ratio and superparamagnetic properties. Immobilized surface ligands capture bacteria, and the MNP-cell complex can then be separated rapidly from even complex solutions (Wang et al., 2015). Carbohydrates are becoming an economical ligand option. Cell surfaces and carbohydrate functional groups form non-covalent, electrostatic forces, similar to the antigen-antibody bonds, which then persist throughout the extraction process. Recent development have found carbohydrates with increased specificity to target bacteria (Shi and Yu, 2012; Yazgan et al., 2014). Electrically-active nanoparticles (EANP) additionally provide more sensitive electrochemical or spectrophotometric detection methods (Duan et al., 2012; Matta et al., 2018; Wang et al., 2017).

Reviewed here are state-of-the-art nano-biosensing methods designed for rapid bacterial extraction using suspended MNP. Selective versus non-selective functional groups are compared with respect to their capture ability. Those MNP methods proven in more complex matrices, which closely replicate food sampling, are also evaluated. Some MNP applications additionally use EANP to intensify optical detection or electrochemical methods. Carbohydrate ligands from a broad spectrum of research areas is discussed with regards to selectivity. Finally, a novel rapid (30 min) MNP-cell-

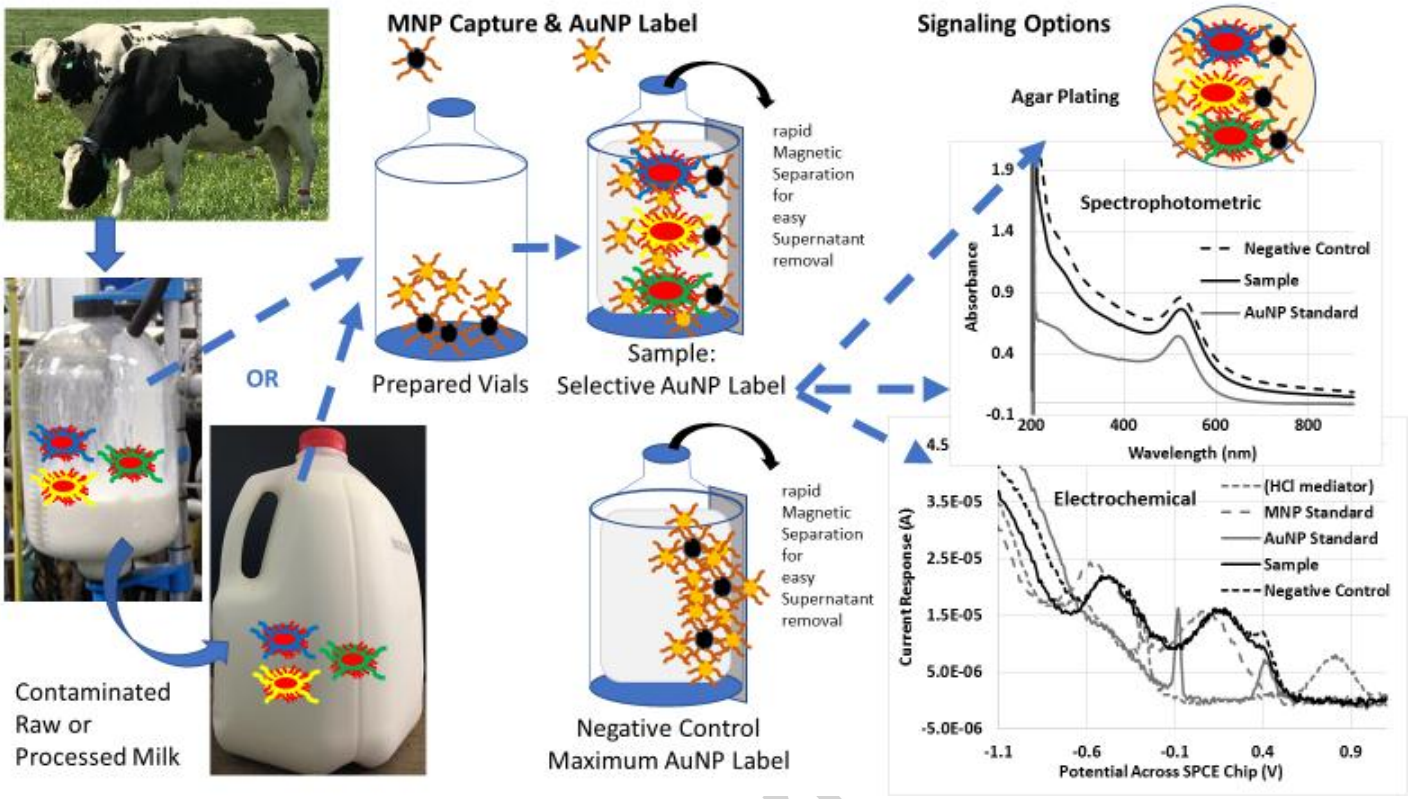

Figure 1. Schematic of the MNP-cell-AuNP biosensor for total bacterial load. Carbohydrate-functionalized MNP extract E. coli from artificially contaminated milk, while dextrin-coated EANP attach to captured cells at different cell receptors. Negative controls consist of sterile milk where MNP-EANP complexes form due to carbohydrate attraction between the functional groups. Cell quantification is possible using FDA bacteriological analytical methods (BAM) agar plating (top), where neither MNP nor EANP inhibit bacterial growth and negative controls will have no cell growth present. Rapid biosensing is possible with spectrophotometric or electrochemical signaling, where negative controls will produce larger signals due to higher EANP presence than samples, due to saturation binding of EANP to MNP.

AuNP nano-biosensing method is introduced that exclusively uses biocompatible carbohydrate ligands immobilized onto MNP and AuNP to detect the presence of *E. coli* in milk using spectral and electrochemical detection, as shown in Figure 1.

2. MNP-assisted Biosensing Properties

Functionalized magnetic nanoparticles (MNP) allow rapid capture and extraction of pathogenic bacteria from liquid matrices in real-time, as well as target concentration with minimal liquid handling. MNP have large surface area to volume ratios, providing for high surface functionalization. Many applications conjugate biological compounds to the MNP surface, such as antibodies or nucleic acid aptamers, to improve their specificity (Bai et al., 2013; Huang et al., 2011; Hwang et al., 2016; Liu et al., 2016; Luo et al., 2012; Mun and Choi, 2015; J. Y. Park et al., 2015; Shim et al., 2014b; Zhiyang et al., 2010) Park et al. MNP-aptamer biosensing shown in Figure 2 was able to visibly detect up to 5 log CFU/mL *Salmonella* (J. Y. Park et al., 2015). But random DNA orientation or antibody cross-reactivity can reduce assay sensitivity (Shim et al., 2014a; Sung et al., 2013; Zhao et al., 2017), as also does matrix interference (Kanayeva et al., 2012).

MNP are synthesized through a variety of methods, including microemulsion, co-precipitation and thermal decomposition, with a variety of final compositions, including iron oxides such as Fe_3O_4 or alloys such as FePt and $CoPt_3$. An excellent review of these synthesis methods was written by Lu et al. (Lu et al., 2007). The aforementioned MNP functional surfactants further protect the nanoparticle from degradation.

Various carbohydrate surfactants have been used as

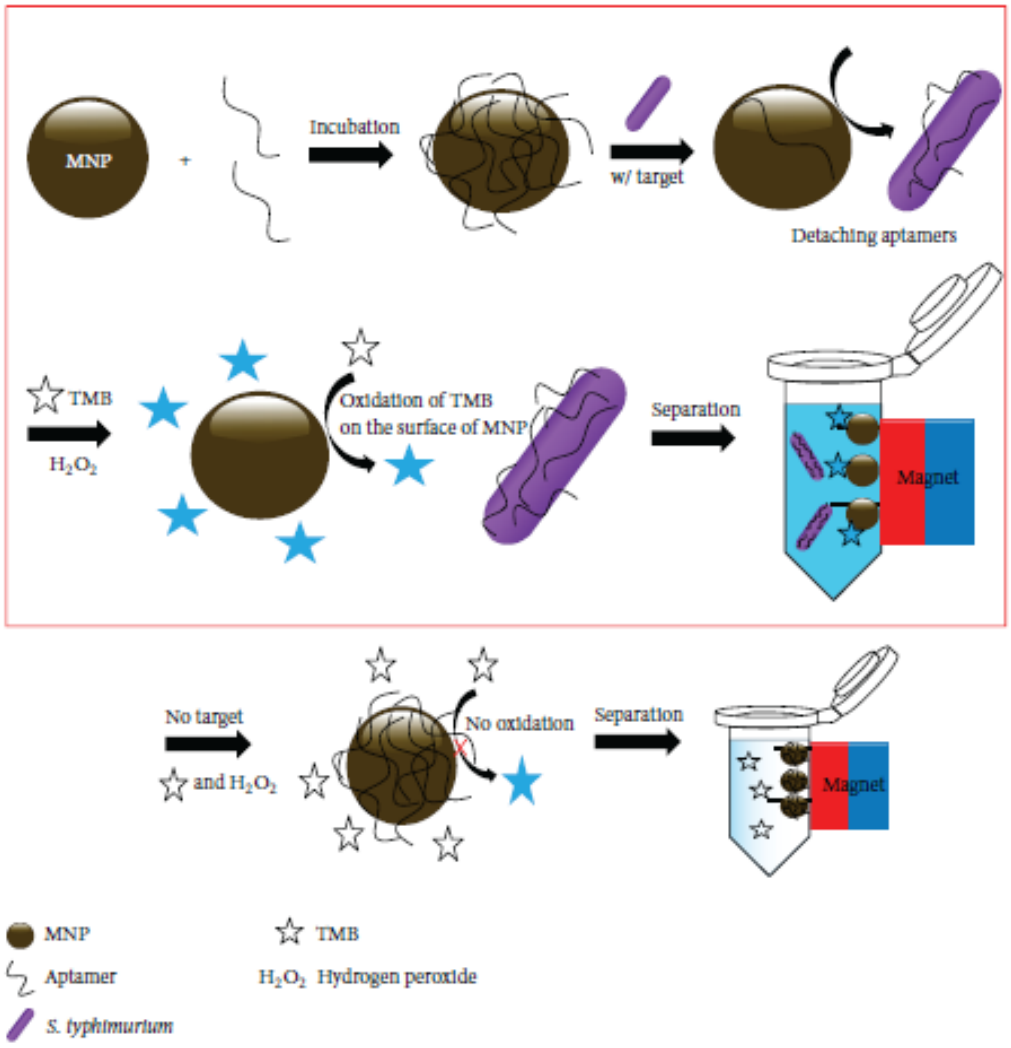

Figure 2. MNP-based colorimetric biosensing scheme to detect bacteria with DNA aptamers (J. Y. Park et al., 2015).

antibody substitutes, making the MNP more biocompatible for biological sample applications. Examples include lectins, mannose, oligonucleotides, galactose, glucose, caprylic acid, cysteine and chitosan (Cho et al., 2017; Dehdashtian et al., 2016; Li et al., 2013; Lin et al., 2002; Raj et al., 2015; Shim et al., 2014a; J. Wang et al., 2016). As a group, carbohydrates retain their structural integrity and chemical reactivity when immobilized onto the surface of MNP. The chemical reactivity of each surfactant then affects MNP suspension and capture dynamics.

Chitosan is a cationic biopolymer derived from chitin with a high percentage of amino groups that aid in MNP suspension. Amino groups improve nanoparticle suspension in aqueous solution (Chang et al., 1997), and improve proximity between biological target and MNP. Galhoum et al. functionalized MNP with chitosan crosslinked to cysteine (Galhoum et al., 2015), further increasing amino group presence. Reactive carboxyl groups can form amide bonds, for example, crosslinking with glutaraldehyde (Fratila et al., 2016; Leitgeb et al., 2014). Oleic acid, citrate, and ethylene glycol are other biocompatible surfactants used on nanoparticles (Basina et al., 2010; Mahdavi et al., 2013; Prasad et al., 2005).

Each carbohydrate displays a different specificity towards biological target epitopes based upon their chemical moieties. Cysteine amino acid has three reactive moieties: carboxyl, ammonium and thiol groups. It was proposed that the carboxyl O and thiol S groups bind to the iron oxide nanoparticle core (R. Ahmadi et al., 2012; Reza Ahmadi et al., 2012), while the positively charged amino group electrostatically binds the highly negative cell surface (Raj et al., 2015). Clues to carbohydrate specificity are found studying human cell epitope binding, which microbial cells also bind during infectious disease initiation. Mannose, glucose and galactose sugars show varying specificities to different cell surface

markers (Fratila et al., 2016; Horák et al., 2007; Sharon et al., 1981), binding the Fim-H surface molecule on *Escherichia coli* (Trungkathan et al., 2014).

Although chitosan is a natural antimicrobial agent (Kong et al., 2010; Mukherjee and De, 2017; Shi et al., 2016), its bonding strength to bacterial cells makes it a desirable MNP surfactant for extraction purposes. Its polycationic structure binds easily to the anionic surface markers of microorganisms (Kong et al., 2010). The expediency of MNP extraction minimizes any deleterious effects. Also at high pH 10, chitosan is negatively charged, but at more neutral conditions such as in many liquid foods (pH 5 to 7) chitosan is more positively charged and more effective in cell attachment (Ge et al., 2009; Kong et al., 2010).

The combination of the selected synthesis method, core composition and surfactant determine the final MNP properties, particularly free space permeability, particle dispersion or aggregation, biocompatibility, and their mechanical and electrochemical stability. MNP magnetization saturation (M_s) properties can be identified using hysteresis magnetization plots (Figs. 3A & 3B), which

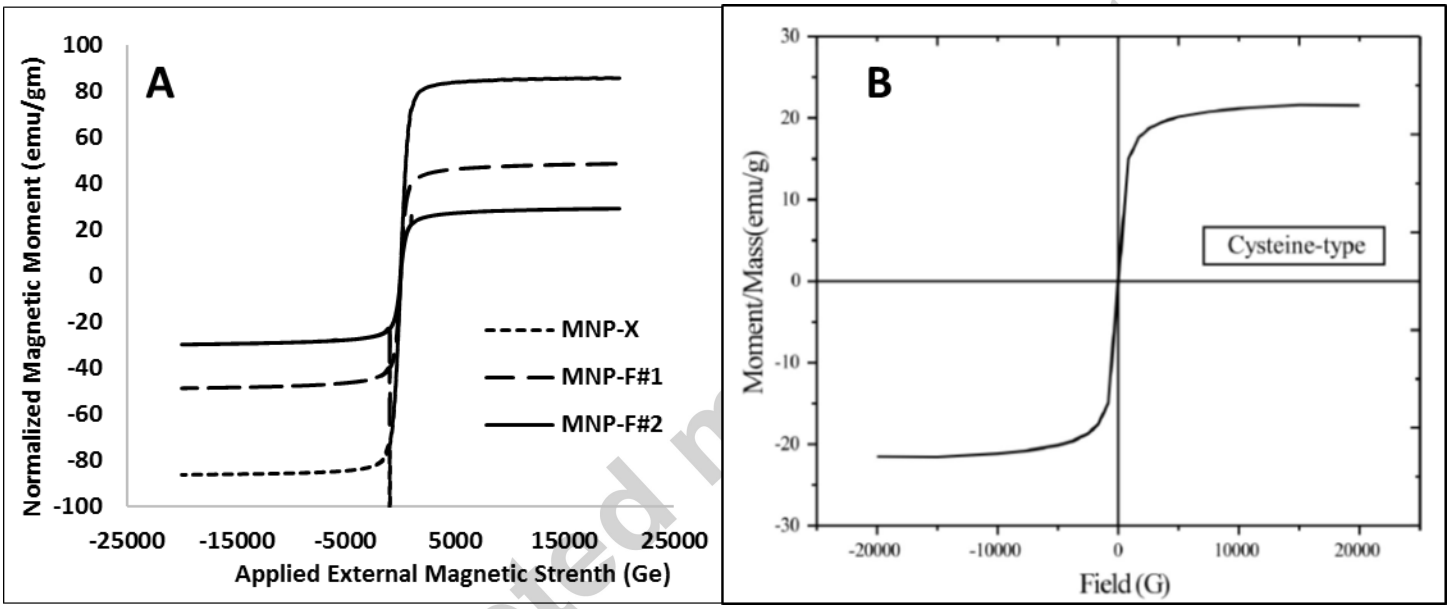

Figure 3. Examples of hysteresis magnetization for magnetic nanoparticles (MNP) functionalized with carbohydrate groups, (A) from Alocilja Nano-Biosensors lab and (B) used in metal recovery *(Galhoum et al., 2015)*.

show that application of an external magnet quickly saturates the nanoparticle magnetic field, aligning the magnetic moments, causing MNP to migrate to the magnetic force (Fratila et al., 2016; Issa et al., 2013; Obaidat et al., 2015). When the applied magnetic field is zero, superparamagnetic nanoparticles do not retain a net magnetic moment. Iron-oxide-MNP display strong superparamagnetism, especially below threshold diameters of 50 nm. These MNP do not aggregate without an external magnet present and therefore MNP are easily suspended evenly into liquid solutions, and following microbial capture, are easily separated from the supernatant upon application of an external magnet. This eliminates the need for time-consuming centrifugation to separate bacteria from food matrices.

Values for MNP M_s vary, due to ferric oxide core diameter and carbohydrate functional group. As shown in Table 1, surfactants reduce the magnetic moment response. For example, MNP prepared by Mahdavi et al. without surfactant showed increasing M_S as their diameter increased, but for the largest 25 nm diameter with oleic acid surfactants, M_S dropped from 81 emu/gm to 58 emu/gm. In addition, defects, or "holes" in the iron core also reduce saturation magnetization values. Therefore, a direct relationship between overall diameter and M_S cannot be expected if other parameters vary. In comparing the carbohydrate-functionalized MNP produced in our Nano-Biosensors Lab against others, the M_S values are relatively strong.

Table 1. Magnetization properties of various magnetic nanoparticles (MNP) with carbohydrate functional groups.

Physical Diameter (nm)	Surfactant (functionalization)	Magnetization Saturation (emu/gm)	Synthesis Method	Author
21	Oleate	17	Thermal Decomposition w/o O_2	(Unni et al., 2017)
21	Oleate	74	Thermal Decomposition w/ O_2	
7.83	None	58	Hydrothermal	(Mahdavi et al., 2013)
8.29		70		
9.41		78		
< 25	None	81		
	Oleic Acid	58		
120	Glutaraldehyde w/ antibody	~ 60	Solvothermal	(Joo et al., 2012)
10	Chitosan-coated	45.09	Coprecipitation	(Sanchez-Ramirez et al., 2017)
8	Chitosan-coated w/ cellulase enzyme	37.58		
(<2000)	Cysteine-glutaraldehyde /Chitosan	1.15		(Abou El-Reash, 2016)
7 – 25, with 150-250 aggregation	Chitosan w/ epichlorohydrin crosslink to cysteine	21.51	Coprecipitation	(Galhoum et al., 2015)
50 – 55	Alginate	59.3	Coprecipitation	(Castelló et al., 2015)
80 – 120	Chitosan	56.8		
18 - 20	None	62	Coprecipitation	(Unsoy et al., 2012)
103	23% Chitosan	39		
58	15% Chitosan	25		
14	Chitosan-FITC fluorescent marker	53	Coprecipitation	(Ge et al., 2009)
14	None	55		
8.5	None	58	Coprecipitation	(Soares et al., 2016)
	Low mw chitosan	29		
	High mw chitosan	18		
8	None	61	Thermal Decomposition	
	Low mw chitosan	30		
	High mw chitosan	25		
5 – 15	(none)	83.87	Coprecipitation	Alocilja Nano-Biosensors Lab, MSU
	Glycan coating	47.06		
	Glycan/cysteine	28.31		

3. Suspended MNP-assisted Biosensing

MNP's ability to extract and detect targeted biological components depends on their magnetization properties and surface functionalization. Table 2 provides detailed information concerning biosensing applications using suspended MNP, functionalized with either selective or non-selective surfactants. Antibody surfactants have higher specificity for their targets, for example against *Listeria monocytogenes* showing a linear detection response between 10^3 to 10^6 colony forming units per mL (CFU/mL (Wang et al., 2017). Jansaento et al. designed a deoxy ribonuclease acid (DNA)/polymerase chain reaction (PCR) method that used aptamer-based MNP that achieved a detection limit of 4 log CFU/mL (Jansaento et al., 2016). Although antibodies, genetic aptamers, and fluorescent tags are selective to their targets, improving assay sensitivity, they are expensive, requiring special preparation and storage (X. Wang et al., 2016; Li et al., 2013; Jansaento et al., 2016; Malic et al., 2015; Kanayeva et al., 2012; Zhang et al., 2014).

Carbohydrate ligands are economical options as MNP surfactants against microbes. Currently many reported carbohydrate ligands are non-selective, but still successfully detect various biological targets. Lin et al. detected 10^1 to 10^8 CFU/mL *E. coli* using MNP-chitosan/glutaraldehyde with wireless magneto-elastic resonance (Lin et al., 2010). Vancomycin-polyethylene-glycol-MNP was used to extract *Listeria*, among other Gram-positive bacteria using UV trans-illumination detection (Meng et al., 2017). Wang et al. used cetyltrimethylammonium bromide coated MNP to recover up

to 1000 ng/L estrogen from pork samples (J. Wang et al., 2016), whereas chitosan-MNP recovered over 90%, or up to 720 μM, morphine from synthetic urine and serum (Dehdashtian et al., 2016). Work in our Nano-Biosensor Lab found glycan-coated-MNP and cysteine/glycan-coated-MNP captured over 70% of microbial contamination directly from undiluted milk, and over 40% from beef juices, orange juice and apple cider (Table S1), providing sufficient bacterial presence for sensitive detection.

A major advantage of MNP is their ability to separate biological targets from their matrices, even concentrating captured bacteria, using only an external magnet. Most of these reported methods were tested in simple buffer or food rinsate solutions such as the *E. coli* detection shown in Figure 4, but food matrix interference was not studied for subsequent detection using refractive index (Liu et al., 2016), fluorescence spectrometry (Wan et al., 2014), or cyclic voltammetry (Pal and Alocilja, 2010). Concentrated MNP-target, though, can improve optical detection (Sung et al., 2013). MNP may even be incorporated into subsequent detection steps, such as interdigitated microfluidic impedance (Kanayeva et al., 2012) or chemiluminescence (Mun and Choi, 2015; Zhiyang et al., 2010) without signal interference. MNP even provided optical signaling in *Salmonella* quantification (Fig. 5).

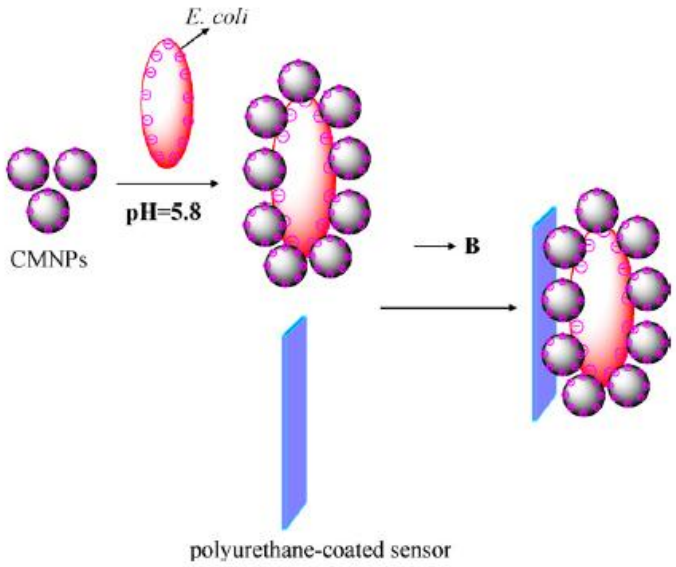

Figure 4. Glutaraldehyde-modified chitosan/MNP capture of *E. coli* with magnetoelastic detection (Lin et al., 2010).

Two pitfalls in suspended MNP biosensing are cross-reactivity against non-target species and matrix interference with detection signaling. Even using selective antibody ligands, *Listeria* detection showed 50% cross reactivity (Zhao et al., 2017) and a *Staphylococcus* assay showed 40% cross reactivity (Sung et al., 2013), both against non-target pathogens. Another MNP-antibody method to detect *Listeria* cross-reacted with *Staphylococcus* (Shim et al., 2014a). Non-selective, carbohydrate surfactants show broad spectrum capture, but vancomycin-PEG-MNP suffered only 20% cross reaction with Gram-negative bacteria (Meng et al., 2017). When food matrices such as beef wash solution or pork extracts were introduced into the sampling method, detection sensitivity was reduced with capture at 70% (Kanayeva et al., 2012). Carbohydrate-functionalized MNP produced in the Alocilja's Nano-Biosensors Lab showed similar matrix interference, but matrix effects were factored in the final signal interpretation using controls.

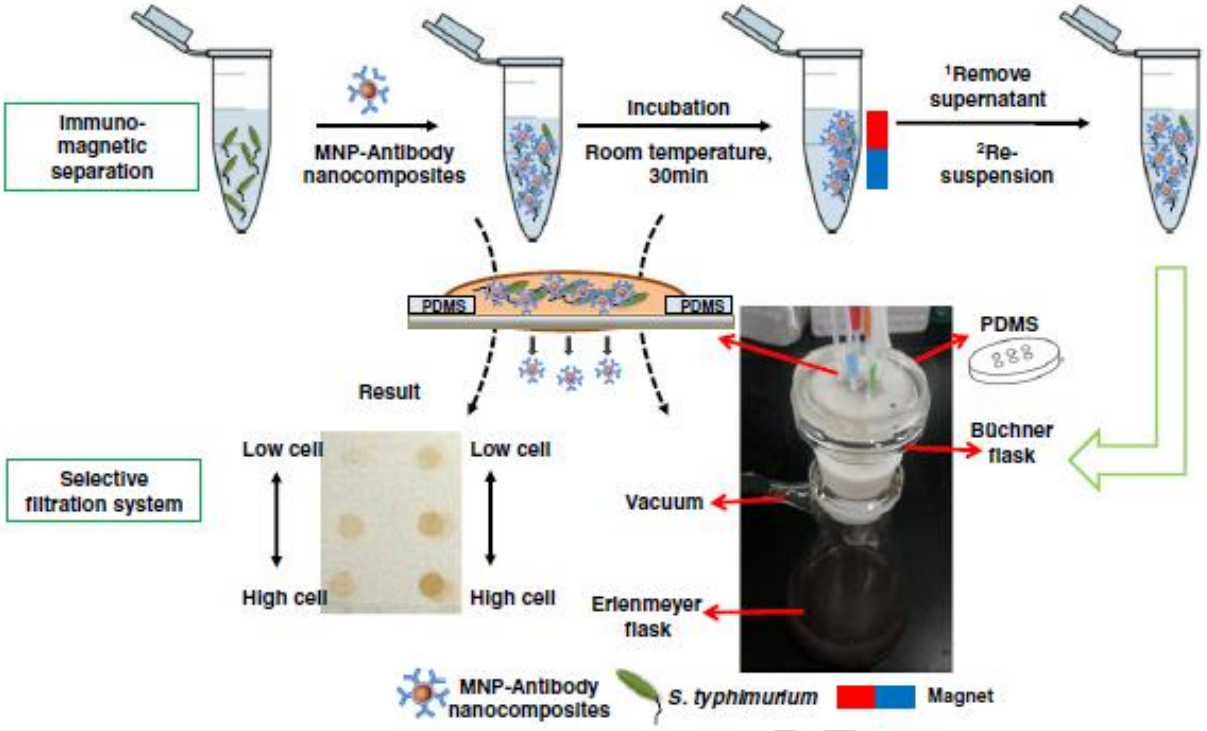

Figure 5. *Salmonella* detection using optical density of vacuum-filtered MNP/Ab-cell complexes (Shim et al., 2014b).

4. Enhanced Biosensing with Electrically-Active Nanoparticles

Electrically-active nanoparticles (EANP) have strong surface plasmon resonance (SPR) properties that make them ideal for nano-biosensing methods. EANP generate local electromagnetic fields through conductance of electrons, detectable by optical, spectral and electrochemical instrumentation. Microbial surfaces labeled with EANP show amplified signaling for higher assay sensitivities and detection limits down to 10^1 CFU/mL. Nanoparticles used in MNP-cell-EANP nano-biosensing (Table 3) include those produced from titanium, gold and other transition metals, yttrium and other rare metals, quantum dots from lead sulfide and silica dots (Duan et al., 2016; Joo et al., 2012; Kuang et al., 2013; Sun et al., 2016; Wang et al., 2017).

AuNP surface plasmon resonance occurs within the UV-visible region between 380 to 780 nm, making them highly suitable as colorimetric biosensors (Contreras et al., 2016; Hormozi-Nezhad et al., 2012; Liu et al., 2015; Sattarahmady et al., 2015; Verma et al., 2015) or microbial concentration can also be determined spectrophotometrically (Lepoitevin et al., 2015). Particles with diameters below 30 nm show absorbance maximums at approximately 520 nm. Other SPR absorbance maximums are 230 nm for titanium oxide nanoparticles (TN) or 630 nm for quantum dots (QD) photoluminesce. Rare earth metal nanoparticles can be designed to fluoresce at varying wavelengths, allowing simultaneous detection of multiple targeted bacteria (Duan et al., 2012).

As with MNP, EANP surface ligands determine their binding properties to targeted biological compounds. Citrate is a conventional surfactant for AuNP (Afshinnia et al., 2017; Hormozi-Nezhad et al., 2012; Shuguang Wang et al., 2011), but other capping agents have been investigated for microbial binding specificity. In evidence of surfactant specificity, cysteine-capped AuNP were able to bind E. coli more effectively than citrate-capped AuNP, purportedly from positively charged amino group attraction to negatively charged microbial surfaces (Raj et al., 2015).

Few reported biosensing methods combine suspended MNP capture with EANP labeling, as shown in Figure 6. Notably, many of the reported methods summarized in Table 3 target Salmonella in their development, using antibody or aptamer ligands on both MNP and EANP with optical or spectral signaling for detection (Duan et al., 2012; Kuang et al., 2013; Sun et al., 2016). In direct signaling, the MNP-cell-EANP complex is directly quantified. For example, Duan et al. (2012) used rare earth nanoparticles functionalized with DNA aptamers to detect *Salmonella* and *Staphylococcus* (10^1 – 10^5 CFU/mL) from filtered environmental water

Table 2. Biosensing methods using suspended functionalized magnetic nanoparticles (MNP).*

MNP Biosensor – Signal Generation	Ligand – Target –Sample Matrix	Linear Range	Reference
Polyurethane-coated Metglas – magneto-elastic sensor loading	Chitosan/ glutaraldehyde – *E. coli* – phosphate buffer	$10^1 – 10^8$ CFU/mL	(Lin et al., 2010)
Impedance from microfluidic interdigitated gold-microelectrode	Antibody – *Listeria* – phosphate buffer and food rinse water	$10^3 – 10^7$ CFU/mL	(Kanayeva et al., 2012)
Ethanol separation – HPLC-DAD	CTAB-coated MNP@caprylic acid – estrogens – pork	5 – 1000 ng/L for standards	(J. Wang et al., 2016)
PFBT dis-placement – fluorescence spectrometry	q-MNP-1, 2, or 3/PFBT – *S. oneidensis, V. fischeri, M. luteus, E. tarda, E. coli. V.alginolyticus, P.aeruginosa,* and *P.pastoris* – phosphate buffer	10^7 CFU/mL	(Wan et al., 2014)
TMB oxidation – absorbance spectrometry	Oligo-nucleotide – *Salmonella* – water	7.5 x 10^5 CFU/mL	(J. Y. Park et al., 2015)
PCTE filtration – HRP chemiluminescence	HRP-MNP-antibody – *Salmonella* – PBS	$10^1 – 10^4$ CFU/mL	(Mun and Choi, 2015)
Vacuum-filtration – optical density	Antibody – *Salmonella* – PBS	$10^1 – 10^4$ CFU/mL	(Shim et al., 2014b)
Vacuum-filtration – optical density	Antibody – *Listeria* – PBS	$10^1 – 10^3$ CFU/mL	(Shim et al., 2014a)
Au-chip loading – SPR	Ab1 & Au-Chip-Ab2 – *Salmonella* – PBS	$10^1 – 10^9$ CFU/mL	(Liu et al., 2016)
Magnetic resonance relaxometry	Antibody – *Listeria* – 2% milk	$10^0 – 10^3$ CFU/mL	(Zhao et al., 2017)
DNA extraction, PCR & gel electro-phoresis – UV transillumination	Vancomycin-PEG – *Listeria* & Gram(+)– PBS & lettuce homogenate	$10^1 – 10^6$ CFU/mL	(Meng et al., 2017)
Enzymatic chemiluminescence of AMPPD	MNP-Ab1 & ALK-Ab2 – *E. coli*	10^3 CFU/mL	(Zhiyang et al., 2010)
Magneto-phoresis separation	Antibody – *E. coli* – PBS	10^3 CFU/mL	(Huang et al., 2011)
CNN membrane separation – resistance	MNP-Ab1 & CNN-Ab2 - *E. coli* – Tris buffer	$10^1 – 10^4$ CFU/mL	(Luo et al., 2012)
PCR & gel electrophoresis – UV transillumination	DNA PCR for *Salmonella & Listeria* – buffer	$10^0 – 10^4$ CFU/mL	(Bai et al., 2013)
LFA inverse color line	ssDNA – *Salmonella* – milk	Above 10^3 CFU/mL	(Hwang et al., 2016)
CA filtration – optical density	Antibody – *Staphylococcus* – PBS and milk	10^3 CFU/mL in PBS and 10^5 CFU/mL in milk	(Sung et al., 2013)
Filtration – ferrocyanide mediated DPV	Chitosan – morphine – PBS or synthetic urine & serum	0.01 – 2 µM and 2 – 720 µM	(Dehdashtian et al., 2016)
PCR amplification – optical HRP enzyme fluorescence	DNA – *Campylobacter* – chicken skin culture	0.1 pg DNA or 10^4 CFU equivalents/ mL	(Jansaento et al., 2016)
CN – electrospun LF biosensor separation – resistance	CMN-mAb & biosensor-pAb – *E. coli* O157:H7 – peptone water	$10^1 – 10^4$ CFU/mL	(Luo et al., 2012)
Electrochemical CV transducer	EAM-Ph-Pro-DNA & SPCE-PRO-bio-DNA – amplified *Bacillus anthracis* DNA in water	Sensitive 0.01 – 10 ng/µL DNA	(Pal and Alocilja, 2010)
TEM analysis	Glycan carbohydrate – *E. coli* O157:H7	(not applicable)	(Lim et al., 2017)
Electrochemical redox ferrocyanide-mediated CV	Chitosan or chitosan/cysteine – *Salmonella, E. coli, Bacillus & Listeria* – PBS, milk, beef juices & apple cider	$10^4 – 10^8$ CFU/mL	Nano-biosensors lab research

* HPLC-DAD = high performance liquid chromatography diode array detection, CTAB = cetyltrimethyl ammonium bromide, PFBT = polymer functionalized with side-chain carboxylic acid group, q-MNP-1, 2 or 3 = quaternized MNP functionalized w/ 3 types of organic bromides, LDA = linear discriminant analysis, TMB = 3,3,5,5-tetramethylbenzidine, PCTE = polycarbonate track-etched filter, HRP = horse-radish peroxidase, PMT = photo-multiplier tube; PBS = phosphate buffered saline, SPR = surface plasmon resonance, Ab1 and Ab2 = monoclonal &/or polyclonal antibodies, Au-chip = gold chip, PEG = polyethylene glycol, Gram(+) = Gram-positive bacteria, Gram(-) = Gram-negative bacteria, PCR = polymerase chain reaction, AMPPD = 3-(2-spiroadamantane)-4-methoxy-4-(3-phosphoryloxy) phenyl-1,2-dioxetane substrate of ALK enzyme, ALK = alkaline phosphatase enzyme, CNN = cellulose nitrate nanofibers, ASMNP = amino-modified silica-coated magnetic nanoparticles, PCR = polymerase chain reaction, DNA = deoxyribonucleic acid, LFA = lateral flow immunoassay, CA = cellulose acetate, DPV = differential pulse voltammetry, CN = cellulose nitrate, LF = lateral flow, CMN = conductive magnetic nanoparticle w/ electrically-active PANi shell, mAb = monoclonal antibody, pAb = polyclonal antibody, CV = cyclic voltammetry, EAM = electrically-active magnetic nanoparticles w/ electrically-active PANi shell, Ph-Pro-DNA = phosphorylated DNA probes, and SPCE-PRO-bio-DNA = screen printed carbon electrode biotinylated DNA probe.

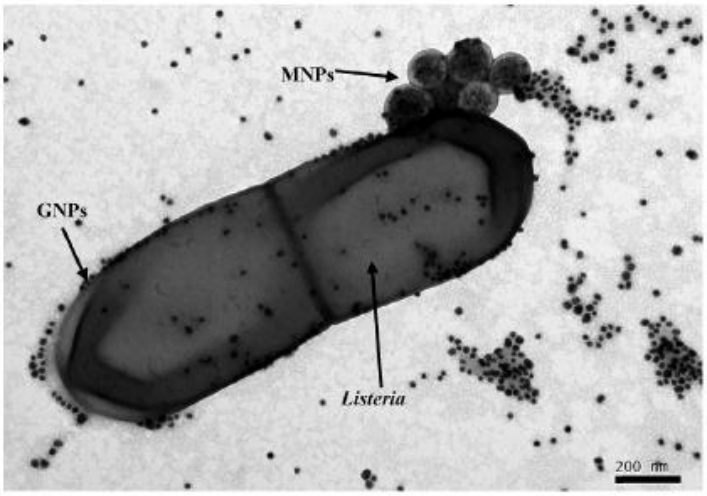

Figure 6. MNP/Ab-Listeria-AuNP/AuNP/urease complex imaged using transition electron microscopy (Wang et al., 2017).

samples (Duan et al., 2012). Inverse methods quantify microbial presence by the level of unbound EANP in the supernatant. Levels of unattached EANP identified *Salmonella* presence (10^2 – 10^5 CFU/mL) in diluted milk with AuNP labeling (Duan et al., 2016), or residual TN quantified *Salmonella* (10^2 – 10^8 CFU/mL) in milk (Joo et al., 2012). AuNP functionalized with both antibody ligand and urease enzyme was used in a biosensing assay shown in Figure 7 that monitored impedance changes to detect *Listeria* (Wang et al., 2017).

Dextrin is a novel capping agent used to reduce gold chloride during AuNP production (Anderson et al., 2011; Bankura et al., 2015). This oligosaccharide improves AuNP/dextrin suspension in aqueous-based solutions by its low molecular weight, pKa of 12.3, and hydroxyl chemical groups. Dextrin is also biocompatible, for example reducing selenium nanoparticle toxicity from 95% against human cells to 15% (Malhotra et al., 2016). Dextrin-capped AuNP developed in our Nano-Biosensors Lab successfully detected *Salmonella* and *E. coli* from undiluted milk in a proof-of-concept design, described below.

Comparison of MNP-cell (Table 2) versus MNP-cell-EANP (Table 3) nano-biosensing methods shows EANP SPR properties improves optical and spectral detection. This advances development of rapid, simple and economical microbial assays, improving subjective visual tests and replacing complicated methods requiring expensive instrumentation. Spectral detection of MNP can mask bacterial presence due to their wide absorbance band (Matta et al., 2018), therefore secondary reactions, such as TMB oxidation (J. Y. Park et al., 2015) or HRP enzymatic chemiluminescence (Mun and Choi, 2015) (Table 2) were required.

All selective and non-selective methods suffer false positive results from cross-reactivity, which minimizes

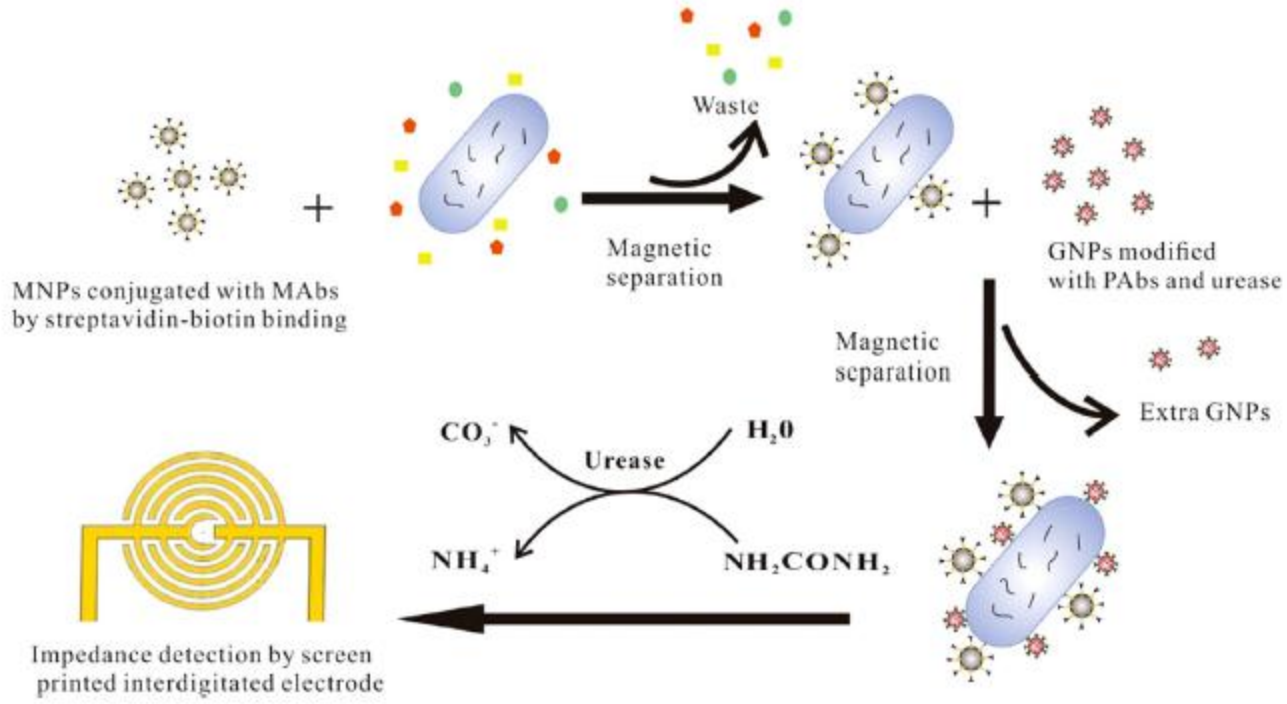

Figure 7. MNP/Ab-Listeria-AuNP/AuNP/urease biosensing with impedance changes from urea production (Wang et al., 2017).

assay efficacy. The trade-off between expensive selective ligands, complicated technology and time-consuming procedures versus economical carbohydrate ligands and user-friendly methods with easily-adapted signaling should be a driving force in improving carbohydrate-based MNP-cell-EANP nano-biosensing.

5. Carbohydrate Ligands Against Microbial Targets

Carbohydrate ligands with selective binding against targeted pathogens can be identified from many sources. Microbial virulence is initiated through bacterial surface protein lectin attraction to tissue carbohydrate ligands. These protein-carbohydrate interactions can be exploited to target pathogens in our food sources. Selectivity can even be improved by addition of binding moieties to the ligand (Haseley, 2002), and synthesis methods are producing a broad range of possible carbohydrate ligands. In 1983, Firon et al. reported that α-glycosides of branched oligosaccharides inhibited type 1 fimbriated *E. coli* attachment to yeast or tissue cells (Firon et al., 1983). Higher monosaccharide numbers in the carbohydrate structure, particularly mannose and fucose, improve multivalent interaction to increase binding strength (Muñoz et al., 2016). Table 4 lists carbohydrates identified through glycobiology or synthesis chemistry.

Several seemingly unrelated review articles have identified selective carbohydrate ligand options. Type 1 fimbriated uropathogenic *E. coli* (EPEC) pathogen was inhibited from binding tissue when monosaccharide bound its terminal α-D-mannoside virulence lectin residue (Lindhorst, 2011). Tissue cell haemaglutinin lectins associated with bacterial virulence were identified by replicating the protein-carbohydrate binding using glycoconjugate receptors (Ramalingam, 2005). Researchers found that C-type lectin immulectin-2 from the tobacco hornworn, *Manduca sexta* binds *E. coli* or *Staphylococcus* lipopolysaccharides, peptidoglycan, and β-1,3 glucan (Shi and Yu, 2012). Even a hospital epidemic identified how *Clostridium difficile* strains acquired the ability to bind and trehalose, a food substitute (Collins et al., 2018).

Carbohydrate ligands offer economical options to larger antibodies and DNA ligands. Fratila et al. reviewed magnetic glyconanoparticles with increased carbohydrate functionalization for rapid cell extraction (Fratila et al., 2016), which is a technique utilized in our Nano-Biosensors lab. Various carbohydrate ligands have shown promising binding properties, as summarized in Table 4. Several of these biosensing methods use mannose or fucose residues (Bader et al., 2016; Baek et al., 2000; Disney and Seeberger, 2004; S. Park et al., 2015; Yazgan et al., 2014), or plant lectins (Safina et

al., 2008; Wang et al., 2013) to target pathogenic bacteria. In addition, the terminal sugar residues of C-type lectins were identified as the primary targets for binding interaction (Shi and Yu, 2012; Uribe et al., 2013).

Protein-carbohydrate bonds identified in Table 4 all use electrostatic forces, similar to those used by antibodies. The *E. coli* Fim-H surface molecule uses hydrophobic binding to attach to mannose-rich oligosaccharides (Yazgan et al., 2014). Hydrogen binding forces are present between

Table 3. Nano-biosensing methods with suspended MNP capture and EANP labeling.*

MNP-cell Labeling – Signal Generation	Ligand – Target – Sample Matrix	Linear Range	Reference
AuNP – optical & absorption spectrometry detection	DNA – *Salmonella* – strained milk	10^2 – 10^5 CFU/mL	(Duan et al., 2016)
TN – absorption spectrometry detection	Ab – *Salmonella* – milk	10^2 – 10^8 CFU/mL	(Joo et al., 2012)
QD w/ photoluminescence spectrometry detection	Ab – *Salmonella* – phosphate buffer	10^3 – 10^8 CFU/mL	(Kuang et al., 2013)
YYbErTmNP – fluorescence spectrometry detection	DNA – *Salmonella* & *Staphylococcus* – buffer	10^1 – 10^5 CFU/mL	(Duan et al., 2012)
Blue-SiNP – visual optical color density confirmation	Ab – *Salmonella* – saline	10^1 – 10^9 CFU/mL	(Sun et al., 2016)
AuNP & urea reaction – supernatant impedance change detection	Ab – *Listeria* – PBS or lettuce wash	10^3 – 10^6 CFU/mL	(Wang et al., 2017)
AuNP w/ DPV detection	Ab – E. coli – PBS	10^1 – 10^6 CFU/mL	(Wang and Alocilja, 2015)
AuNP w/ electrochemical ferrocyanide-mediated DPV or spectrometry detection	glycan/cysteine & dextrin carbohydrates – *Salmonella* & *E. coli* – PBS & milk	10^5 – 10^6 CFU/mL	(reported in this publication)

*AuNP = gold nanoparticles, DNA = deoxyribonucleic acid, TN= titanium oxide nanoparticles, Ab = monoclonal or polyclonal antibody, CFU = colony forming units, QD = quantum dot, YYbErTmNP = (rare earth metals) yttrium ytterbium erbium thulium nanoparticle, Blue-SiNP = silica nanoparticles functionalized with Reactive Blue 14, and DPV = differential pulse voltammetry.

Table 4. Carbohydrate functional groups used to bind biological targets in nano-biosensing methods.

Carbohydrate Ligand – Modifications	Microbial Target – Surface Epitope	Binding Details	Figure & Reference
Mannose-containing oligosaccharides – PTAM, PCAM, DAMP, glucosamine & chitosan	*E. coli* – FimH	Hydrophobic phenyl residues & aliphatic side groups	(Yazgan et al., 2014)
Organic polymer glycopolythiophene – mannose	*E. coli* HB101 – Type 1 piliated	Multivalent polymer acidic group electrostatic bonding and mannose hydrogen binding	(Baek et al., 2000)
Monovalent α-D-mannose-pyranoside – fluorescent DBD dye	*E. coli* DH5α – FimH	(not addressed)	(Bader et al., 2016)
Plant-based lectins ConA, LCA, WGA, MAL, & UEA;	*Campylobacter jejuni & Helicobacter pylori* – lysed cells LPS (ConA & LCA to mannose & glucose, WGA & MAL to β-*N*-acetylglucosamine, UEA to fucose)	Binding requires Ca^{2+} & Mn^{2+} ions	(Safina et al., 2008)
Atlantic *Salmo salar* C-type lectin SSL	*Aeromonas salmonicida* – LPS (mannose-binding) and glycans w/ terminal GlcNAc; also binds *Pseudomonas fluorescens, A. hydrophilia, Pichia pastoris, & Saccharomyces cerevisiae*	Hydrogen binding between 3 to 4 sugar hydroxyl groups to LPS acidic and amino acid side chains (Ca^{2+} coordinated)	(Uribe et al., 2013)
Plant-based lectins from WGA, Con A, UAE, PNA & MAL	*E. coli* O157:H7 – surface mono- & oligosaccharide polysaccharide structures	SEM imaging of WGA-coated biosensor surface with captured *E. coli* cells	(Wang et al., 2013)
Fucose-bearing oligosaccharides Le^b & blood group H type 1 FMNP	*H. pylori* J99 – BabA cell surface fucose binding adhesin lectin	Monomeric sugar binding to protein	(S. Park et al., 2015)
Hemocyte cell surface purified immulectin-2 C-type lectin (w/ extended terminal carbohydrate loop)	*E. coli* K12 & *E. coli* 011:B4 – LPS; *E. coli* K12, *Staphylococcus aureus* & *Bacillus subtilis* – peptidoglycan; *Saccaraomyces cerevisiae* – zymosan & mannan; laminarin (β-1,3-glucan)	Glutamate-proline-asparagine motif binds sugar motifs	(Shi and Yu, 2012)
Mannose monosaccharide – ethanolamine linker to immobilize on microarray	*E. coli* ORN178	(not addressed)	(Disney and Seeberger, 2004)
20 D-mannose derivatives (sulfonamides & cinnamides)	*Pseudomonas aeruginosa* – LecB (PA-IIL) surface lectin virulence factor	Three hydroxy groups from trisaccharide $Lewis^a$, w/ ability to target adjacent protein cleft	(Sommer et al., 2015)
Tridecafullerenes – 120-count mannose residues attached to azide-substituted glycofullerene scaffold & alkyl chain linkers	EBOV infection – DC-SIGN lectin	DC-SIGN recognizes multivalent sugar residues on oligosaccharides	(Muñoz et al., 2016)

* PTAM = p-thiolphenylaminomannose, PCAM = p-carboxyphenylaminomannose, DAMP = 1-deoxy-1-aminomannopyranoside, SPR = surface plasmon resonance, FimH = mannose-specific fimbrial lectin adhesin molecule, H = hydrogen, DBD = [1,3]dioxolo[4,5-f][1,3]benzodioxole, ConA = Concanavalin A, LCA = Lens culinaris agglutinin, WGA = Wheat Germ agglutinin, MAL = Maackia amurensis lectin, UEA = Ulex europaeus agglutinin, LPS = lipopolysaccharides, SSL = Salmo salar lectin, GlcNAc= N-acetylglucosamine, PNA = Arachis hypogaea peanut agglutinin, MAL = tree species Maackia amurensis leukagglutinin,, SEM = scanning electron microscopy, Le^b = Lewis b, FMNP = fluorescent magnetic nanoparticles, BabA = blood group antigen binding adhesin A, and DC-SIGN = dendritic cell-specific intercellular adhesion molecule-3-grabbing non-integrin receptor.

sugar hydroxyls and amino acid residues in microbial surface C-type lectins (Shi and Yu, 2012; Uribe et al., 2013). Type 1 piliated *E. coli* HB101 attached organic polymer through multivalent acidic and mannose hydrogen bonds (Baek et al., 2000). Some binding schemes also require cation cofactors Ca^{2+} or Mn^{2+} for binding between surface lipopolysaccharides and lectins.

6. Microbial Surface Epitopes for Carbohydrate-functionalized MNP-cell-AuNP Nano-biosensing

Microbial pathogens have two main goals: survival and reproduction. A pathogen's survival necessitates its ability to attach, either to surfaces or host organisms; involves secretion of toxins against competitors and regulatory cells; and requires uptake of nutrients for growth, regeneration and reproduction. Microbial cell surfaces are enveloped with molecular structures that fulfill their cellular functions. All of these same microbial surface markers, or epitopes, may also

be used to target those microbes that contaminate our environmental and food supply sources. The human immune system itself produces antibodies and

complement that target pathogen epitopes. Following is a brief review of these microbial epitopes which can be targeted by carbohydrate ligands in nano-biosensing assays.

Microbial surface epitopes may be attached directly to the membrane surface, transverse the membrane to connect external and internal cellular spaces or are in "association" with the cell surface through non-covalent forces. These molecules are complex, frequently constructed from several sub-structures excreted to the cell surface. Epitopes are temporal structures, changing over time with growth and environmental conditions. Due to the complex nature of surface epitopes, many regions along the structure which are not necessarily used in cellular processes may provide novel areas for selective MNP targeted capture.

Nanoparticles can be functionalized with surfactants that target microbial surface epitopes for extraction and quantification from liquid foods. In immune responses, antibody binding is one of the most specific and strongest non-covalent binding mechanisms in cellular processes (Sinha et al., 2002). But antibody ligands are quite expensive and time-consuming to produce and require special handling. Current carbohydrate ligands, such as those summarized in Table 4, are less selective in their binding targets, but have proven their ability to attach to a broad spectrum of surface epitopes at fractions of the cost of antibodies and DNA. Plus, more selective carbohydrate ligands are being discovered and synthesized.

Lipopolysaccharide (LPS) and peptidoglycan moieties make up a substantial amount of prokaryotic cell wall structure. Gram-negative cell walls contain higher amounts of LPS, whereas Gram-positive cell walls are composed of a thick layer of peptidoglycan. LPS is toxic to the human body (Kulshin et al., 1991) and cause antibody immune responses. LPS is composed of a hydrophobic lipid A region, responsible for toxicity, which anchors the structure within the cell membrane, followed by a core polysaccharide region, extending into the O-antigen domain which consists of repeated polysaccharides (Fig. 8, (Galdiero et al., 2012)). Peptidoglycan is composed of sugars and amino acids, with residues of N-acetyglucosamine or N-acetylmuramic acid. Peptidoglycan moieties can be further conjugated to secondary cell wall polymers (SCWP), covalently link to the exposed N-terminus (Candela et al., 2011).

Spread across the cell walls of all microbial types are peptidases and outer membrane proteins that assist in nutrient flow, pathogenesis, motility and cell wall turnover. Peptidases are specialized proteins secreted to the surface that interact with surface carbohydrates and lipids and act as enzymes with catalytic sites involved in peptidoglycan modification, cell wall turnover and cellular locomotion (Joys, 1985; Tran et al., 2010). Adenosine triphosphate (ATP)-binding cassettes (ABC) are one major group of nutrient transporter proteins. Due to the ABC structure specificity among microbial species they are strong antigens, or targets, for immunogenic responses, resulting in highly selective antibodies (Muller et al., 2005). Outer membrane proteins (OMP) are porins that transverse the cell wall providing entry across the cell wall for a broad spectrum of nutrient exchange (Galdiero et al., 2012; Nikaido, 2003)), using active-transport of nutrients at low-

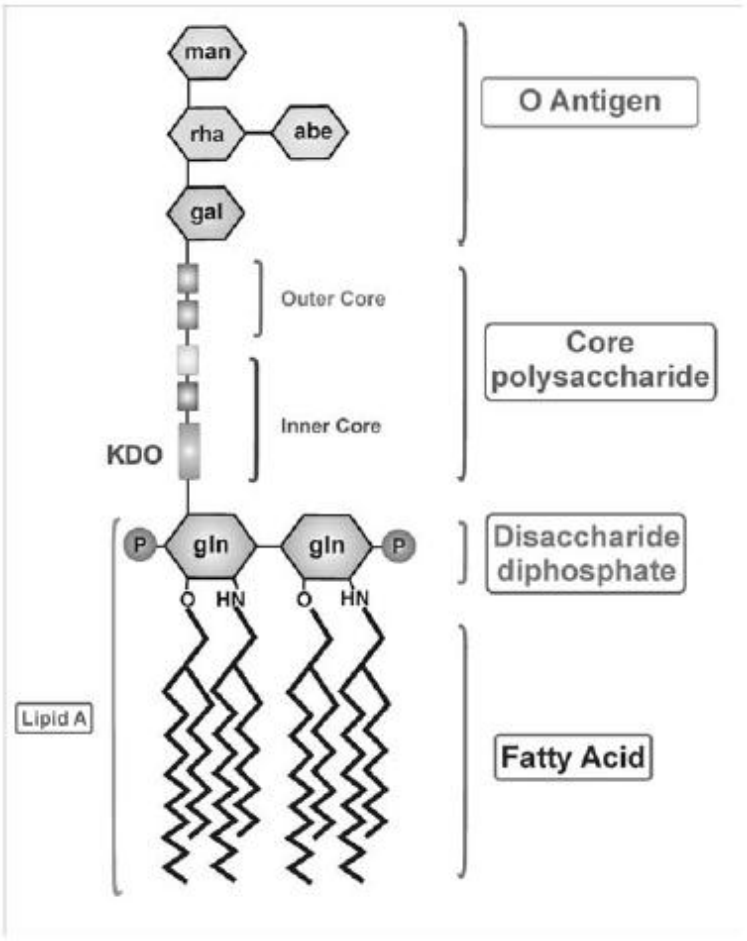

Figure 8. Lipopolysaccharide structure *(Galdiero et al., 2012).*

concentration, and more passive diffusion of higher-concentration nutrients. Due to porin discriminatory transport of hydrophilic compounds by size and charge, they are targets of specific antibody production, especially for OmpD porins (Diaz-Quiñonez et al., 2004; Gil-Cruz et al., 2009; Koebnik et al., 2000).

Microbial cells detect their environment through their cellular wall molecular components. Chemotaxis proteins sense signals secreted from other microbes, OmpC porins sense changing osmolarity, and MSCRAMM (microbial surface components recognizing adhesive matrix molecules) recognize connective tissue of mammalian tissue (Chagnot et al., 2012; Gohar et al., 2008; Singh et al., 1995). Flagella are locomotive organelles attached to the surface of the microbe, composed of monomeric polypeptides with high variability in their protein composition with high specificity per microbial species as H antigens in immuno-reactivity serotyping (Joys, 1985; McDonough, 1965; Piette and Idziak, 1991). Curli and fimbriae are hair-like projections involved in adhesion to surfaces and aggregation with other cells, containing hydrophobic amino acids lysine, proline, and serine, as well as a mannose-binding region (Collinson et al., 1996; Jain and Chen, 2007; Kukkonen et al., 1998; Lin et al., 2002; Stahlhut et al., 2009; Waalen et al., 1983). Pili also acts in surface binding through hydrophobic amino acids that act (Desrosier and Lara, 1981; Korhonen et al., 1980; Neeser et al., 1986; Oxaran et al., 2012; Pratt and Kolter, 1998; Xu et al., 2013).

As major nutrients, amino acid and sugars uptake is facilitated by transporter structures. Cysteine transfer across the cell membrane is performed in cystine form for *E. coli* (Berger and Heppel, 1972), *Bacillus subtilis* (Burguiere et al., 2004), and *Listeria monocytogenes* (Xayarath et al., 2009). Glycosylated milk compounds inhibited lectin proteins of *Pseudomonas aeruginosa* from galactose, fucose and mannose uptake (Lesman-Movshovich and Gilboa-Garber, 2003). *Chronobacterium violaceum* lectin binding protein binds both fucose and mannose, but at different protein orientations (Pokorná et al., 2006).

Chitosan is a polycationic polysaccharide derived from acetylated chitin that easily binds the negative charged surfaces of microbial species, such as seen for *E. coli, Pseudomonas,* and *Salmonella* (Helander et al., 2001; Mellegard et al., 2011). The positively charged amino groups of chitosan also bind *Bacillus* vegetative cells to block nutrient uptake (Fernandes et al., 2009; Manni et al., 2010).

Binding is the transduction event in biosensing that leads to signaling. Electrostatic forces dominate the binding dynamics between targeted microbial cells to dextrin-coated gold nanoparticles (d-AuNP), and to carbohydrate-functionalized magnetic nanoparticles (MNP). Attachment mechanisms are of varying selectivity. The bonds formed during MNP-cell-d-AuNP nano-biosensing described in the following section (Figs. 9A & B) between the cells and the carbohydrate functional groups are non-covalent, electrostatic forces in form, similar to the antigen-antibody bonds (Fig. 6), but of lower strength and specificity. Dextrin's negatively charged hydroxyl groups potentially bind to positively charged amino acid pockets of the cellular surface molecules, leading to seemingly selective attachment of d-AuNP on *E. coli* cell surfaces (Fig. 9A). MNP bind readily to cells and appears to be selective, and d-AuNP also easily bind the MNP functional groups at saturation levels. d-AuNP saturated binding to the MNP (Fig. 9B), though, are potentially between the hydroxyl groups of the dextrin to the high number of positively charged amines in the MNP carbohydrates. Cell presence reduces d-AuNP presence in MNP-cell-d-AuNP complexes from selective binding of d-AuNP to the cell and impedes binding of d-AuNP to the MNP surface.

7. Carbohydrate-functionalized MNP-cell-AuNP Nano-Biosensing

A proof-of-concept study using carbohydrate-functionalized (glycan/cysteine-coated) magnetic nanoparticles (MNP-F#2) and dextrin-coated gold nanoparticles (d-AuNP) was carried out in undiluted vitamin D milk to demonstrate rapid detection using both spectrometry and electrochemical detection. These economical carbohydrate-based nano-biosensors currently show broad selectivity in pathogen detection for total load of bacterial contamination present. As more selective carbohydrate ligands are designed, they can easily be applied to this method with little increase in detection costs.

E. coli C3000, as a model microbe strain, was obtained from the Nano-Biosensors Lab at Michigan State University. The colonies from frozen (-70 ^{o}C) culture were grown on tryptic soy agar (TSA). A single colony was isolated, inoculated into tryptic soy broth (TSB, Sigma-Aldrich, St. Louis, MO) and grown overnight at 37 ^{o}C. One milliliter (ml) of the liquid culture was transferred to a new tube of TSB (9 mL) and incubated at 37 ^{o}C for 4 hours before each experiment. Tenfold serial dilutions of the bacterial culture, from 10^0 to 10^6 colony forming units per milliliter (CFU/mL), were prepared using phosphate buffered saline (PBS, pH 7.4, Neogen, Lansing, MI) before each experiment. Separate similar tenfold dilutions were made in Vitamin D milk (purchased from local commercial seller) from 10^0 to 10^{10} CFU/mL. Culture diluted in PBS and milk was plated on CHROMagar^{TM} *E. coli* (DRG International, Springfield, NJ), incubated overnight at 37 ^{o}C, and enumerated to determine cellular concentration.

Both MNP-F#2 and d-AuNP, herein referred to as MNP and AuNP, respectively, were used as received from the Nano-Biosensors Lab, MSU (Anderson et al., 2011; Wang and Alocilja, 2015). Concentrated AuNP was prepared by removing excess dextrin and solution. A volume of 250 μL of the original AuNP suspension were transferred to 2 mL pinched-tip centrifuge tubes, sonicated for 10 min, and centrifuged at 15,000 rpm at 4 ^{0}C for 20 min. Following supernatant removal, the remaining 20 μL AuNP pellet was sonicated for 15 min to evenly distribute the concentrated AuNP evenly, referred to as "AuNP250". Tubes were stored at 4^{o}C and used within 24 hours of preparation.

MNP were previously proven in-lab to capture microbial cells within a complex milk matrix at over 70% (log CFU/mL basis, Table S1). Cell culture serially diluted in milk (50 μL) was simultaneously exposed to MNP (50 μL of 5 mg/mL prepared in buffer) and AuNP250, plus 100 μL PBS for 30 min, magnetically separated and re-suspended in 100 μL PBS for electrochemical detection or 1000 μL PBS for spectral detection. Negative controls followed the same procedure except without cells.

Spectral absorbance was measured between 900 nm to 200 nm wavelength. Peak absorbances for MNP (620 nm) and AuNP (520 nm) were monitored. All spectra were numerically step integrated between 900 to 220 nm. Averaged MNP-cell-AuNP sample integrations were compared to averaged negative controls (n = 3).

Electrochemical detection was carried out with differential pulse voltammetry (DPV) using a handheld potentiostat (model PG581 Uniscan Instruments, Bio-Logic Scientific Instruments, Seyssinet-Pariset, France), driven by UiE Chem Software. Each test used a disposable screen-printed carbon electrode (SPCE, Gwent Electronic Materials Ltd,

United Kingdom; 1 cm^2 surface area) loaded into the port of the potentiostat. MNP-cell-AuNP were magnetically separated and resuspended in 100 µL 1 M HCl, reacted for 5 min, then the entire contents were applied to the SPCE. Samples were oxidized at 1.2 V for 120 s. DPV was run between +1.2 V to -1.2 V, applied across the electrode, at a scan rate of 17 mV/sec with 5 mV increments for 300 ms step time. A DPV voltammogram was recorded for each sample. All sampling was done room temperature. Maximum absolute AuNP current response was determined between 0.3 V to 0.5 V. Averaged sample peak currents were compared to averaged negative controls (n=3).

This proof-of-concept design on average distinguished between samples with cells present and negative controls for either spectral (Fig. 10A for 3 log CFU/mL) or electrochemical DPV signaling (Fig. 10B for 5 log CFU/mL) ($p < 0.2$) using a one-step simultaneous capture-n-label process in undiluted milk. Binding dynamics were covered in the previous section. AuNP attachment to cells is seemingly selective (Fig. 9A) while it saturates the MNP surface (Fig. 9B), while cell attachment limits the AuNP exposure to the MNP surface. This binding pattern results in higher signaling for negative controls (MNP-AuNP) than for samples (MNP-cell-AuNP).

Reproducibility within the sample replicates is lower (greater standard deviation) than negative controls in both detection methods, as well as low separation (Figs. S1A & B). This is due mostly to the tight signaling response for the given assay conditions, which will be addressed in

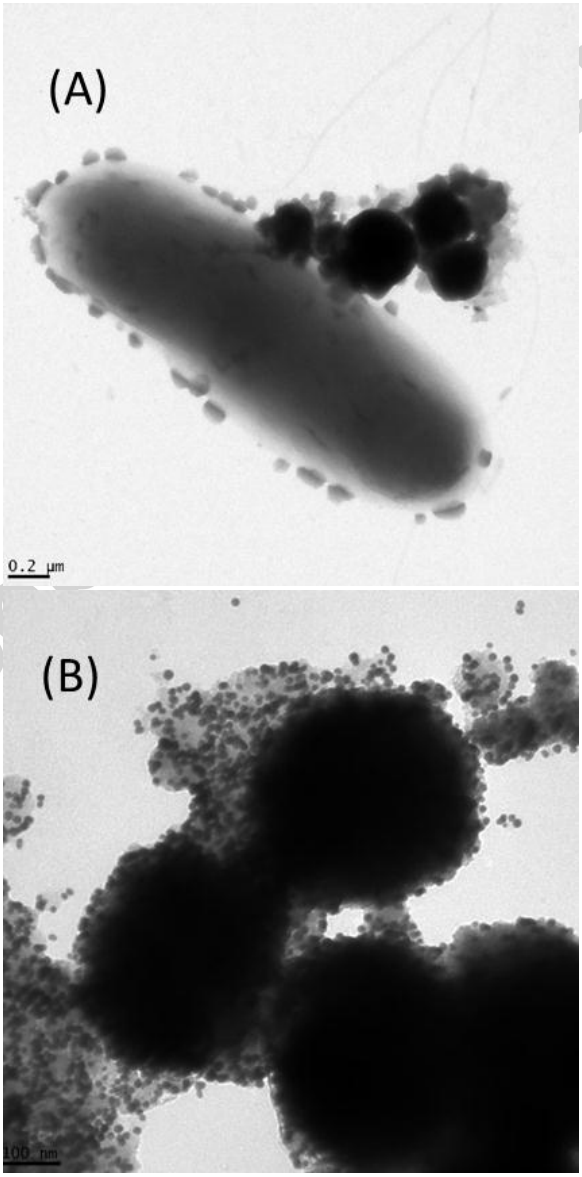

Figure 9. d-AuNP and MNP attachment to *E. coli* cells, forming MNP-cell-AuNP (sample) (A) and MNP-AuNP (negative control) complexes (B).

future method optimization. Particularly for samples, though, cell sizes are much greater than nanoparticle sizes, showing the robust MNP extraction properties. But in the current method, a difference of just 1% (log basis) in MNP capture results in larger signaling shifts for samples due to the more selective binding of AuNP to the cell surface.

Future work will focus on optimizing the assay to improve sensitivity of the tests in microbial detection. During early development work in PBS, the AuNP peak was clearly visible in spectrometry and DPV detection. But in milk, the MNP-cell-AuNP peaks are masked since milk components also attached to both MNP and AuNP (Fig. S1).

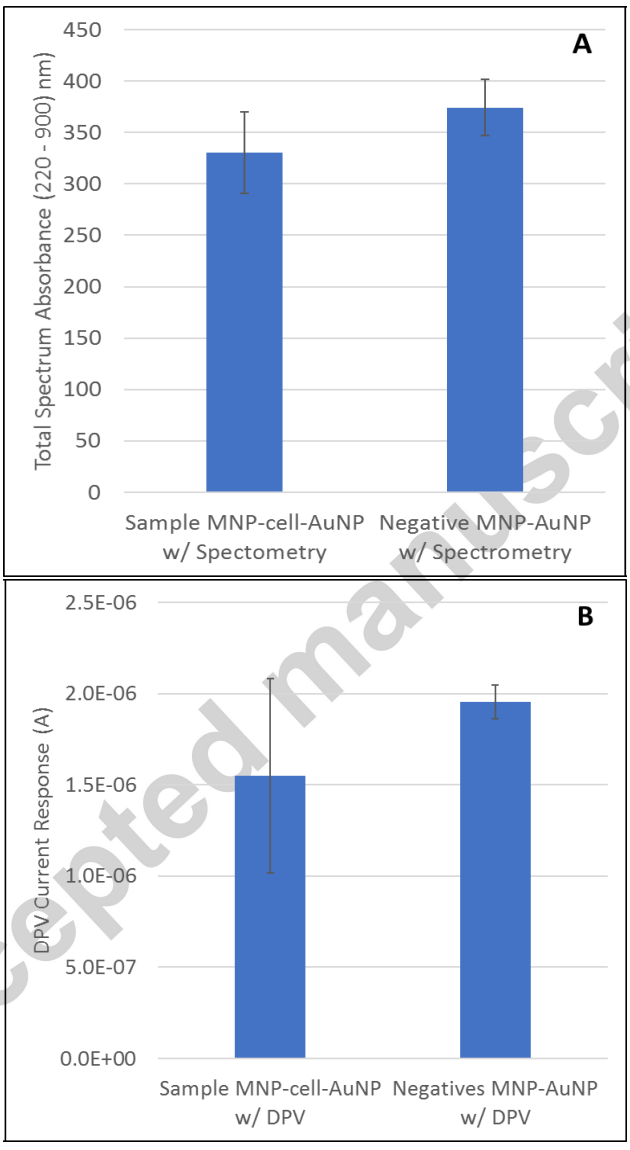

Figure 10. MNP-cell-AuNP nano-biosensing detection of *E. coli* C3000 contamination in milk using 1-step, simultaneous MNP capture and AuNP labeling, where on average spectral signaling distinguished between 3 log CFU/mL cells and negative controls (A), while electrochemical DPV signaling distinguished between 5 log CFU/mL cells and negative controls (B) ($p<0.5$)..

Therefore, sample analysis for spectral absorbance was performed through step-integration. Milk also reacts with HCl in DPV tests, therefore, the HCl volume must be optimized per particular liquid food matrix. In addition, negative controls are required each to ensure direct comparison with samples. As more selective carbohydrate ligands are identified, such as work highlighted in Table 4, greater specificity will improve limits of detection. This rapid, economical MNP-cell-AuNP biosensing method can easily be applied to other liquid foods which would improve food safety through affordable rapid detection.

8. Conclusions

Carbohydrate functionalized MNP are an economical means to expedite microbial extraction in mere minutes from simple and complex matrices such as milk, without the need for time-consuming centrifugation from large sample volumes. Upon extraction, MNP-cell complexes can be concentrated to less than 1 mL, resulting in stronger detection signaling. Although the initial carbohydrate ligands reported here bind and extract the total bacterial load present in samples, higher selectivity is possible through study of the cell surface molecular structures against a range of carbohydrates. Biocompatible ligands are desired as antibody-replacements due to the cost of antibodies, particularly given the persistence of cross-reactions with non-target microbes. Regardless of the ligand used, though, it was shown that several methods were able to significantly quantify microbial presence with the MNP still attached to their target.

Beyond the potentially intensified microbial biosensing via MNP concentration, EANP labeling, such as with quantum dots, TN or AuNP, of the MNP-cell complexes further improves test sensitivity with less complicated spectral and electrochemical detection methods. Microbial contamination along the food supply chain could be detected quickly using this economical method in frequent product checks, assuring suppliers the safety of their product and reducing substantially consumer illness. Additionally, functionalizing MNP and AuNP with inexpensive biocompatible carbohydrates, such as dextin, further decreases assay costs, while reducing hazardous waste production through green chemistry.

Combining carbohydrate-functionalized MNP cell capture and concentration, along with dextin-coated AuNP labeling resulted in promising nano-biosensing development towards the goal of feasible, less complicated tests. Much work in nano-biosensing development has focused heavily on designing highly specific, one-time-use "strip" sensors that involve substantial technology to produce. These are not cost-effective for many worldwide food suppliers, though. Even many of the suspended MNP/EANP biosensing assays reviewed here are still out of reach for many users, requiring special storage or highly technical equipment.

Carbohydrate ligands are easily incorporated onto nanoparticles, and require little special handling, showing a long shelf life at room temperature. As more selective carbohydrate ligands are identified and incorporated into MNP-cell-AuNP assays, consumers can be assured of safer food supplies at affordable costs. While the proof-of-concept test presented here requires optimization for detection at lower cell concentrations, it was successful in detecting *E. coli* presence directly from milk, whereas many reported tests were studied only in simple buffer solutions. The future in nano-biosensing is not in developing more technically complex sensors, but applying technological know-how to develop inexpensive, user-friendly microbial assays.

Acknowledgments

This research was supported by the Alocilja Nano-Biosensors Lab and the Axia at Michigan State University.

References

Abou El-Reash, Y.G., 2016. J. Environ. Chem. Eng. 4, 3835–3847.

Adegoke, Y., 2017. [WWW Document]. News4Jax. URL http://www.news4jax.com/news/international/un-half-of-worlds-population-growth-likely-to-be-in-africa (accessed 6.27.17).

Afshinnia, K., Sikder, M., Cai, B., Baalousha, M., 2017. J. Colloid Interface Sci. 487, 192–200.

Ahmadi, Reza, Gu, N., Hosseini, H.R.M., 2012. Nano-Micro Lett. 4, 180–183.

Ahmadi, R., Ranjbarnodeh, E., Gu, N., 2012. Mater. Sci.-Pol. 30, 382–389.

Anderson, M.J., Torres-Chavolla, E., Castro, B.A., Alocilja, E.C., 2011. J. Nanoparticle Res. 13, 2843–2851.

Bader, D., Klier, D.T., Hettrich, C., Bier, F.F., Wessig, P., 2016. Anal. Methods 8, 1235–1238.

Baek, M.-G., Stevens, R.C., Charych, D.H., 2000. Bioconjug. Chem. 11, 777–788.

Bai, Y., Song, M., Cui, Y., Shi, C., Wang, D., Paoli, G.C., Shi, X., 2013. Anal. Chim. Acta 787, 93–101.

Bankura, K., Rana, D., Mollick, M.M.R., Pattanayak, S., Bhowmick, B., Saha, N.R., Roy, I., Midya, T., Barman, G., Chattopadhyay, D., 2015. Int. J. Biol. Macromol. 80, 309–316.

Basina, G., Panagiotopoulos, I., Devlin, E., Hadjipanayis, G., Colak, L., Hadjipanayis, C., Mao, H., Diamantopoulos, G., Fardis, M., Papavasileiou, G., Niarchos, D., Tzitzios, V., 2010. MRS Proc. 1256.
Beach, C., 2016. [WWW Document]. Food Saf. News. URL http://www.foodsafetynews.com/2016/06/u-n-officials-say-food-safety-is-entwined-with-food-security/ (accessed 6.28.17).
Berger, E.A., Heppel, L.A., 1972. J. Biol. Chem. 247, 7684–7694.
Burguiere, P., Auger, S., Hullo, M.F., Danchin, A., Martin-Verstraete, I., 2004. J. Bacteriol. 186, 4875–4884.
Candela, T., Maes, E., Garenaux, E., Rombouts, Y., Krzewinski, F., Gohar, M., Guerardel, Y., 2011. J. Biol. Chem. 286, 31250–31262.
Castelló, J., Gallardo, M., Busquets, M.A., Estelrich, J., 2015. Colloids Surf. Physicochem. Eng. Asp. 468, 151–158.
Chagnot, C., Listrat, A., Astruc, T., Desvaux, M., 2012. Cell. Microbiol. 14, 1687–1696.
Chang, K.L.B., Tsai, G., Lee, J., Fu, W.-R., 1997. Heterogeneous N-deacetylation of chitin in alkaline solution. Carbohydr. Res. 303, 327–332.
Chen, L., Mungroo, N., Daikuara, L., Neethirajan, S., 2015. J. Nanobiotechnology 13, 45.
Cheng, M.S., Lau, S.H., Chow, V.T., Toh, C.-S., 2011. Environ. Sci. Technol. 45, 6453–6459.
Cho, S., Shin, H.Y., Il Kim, M., 2017. Biointerphases 12, 401.
Collins, J., Robinson, C., Danhof, H., Knetsch, C.W., van Leeuwen, H.C., Lawley, T.D., Auchtung, J.M., Britton, R.A., 2018. Nature 553, 291–294.
Collinson, S.K., Clouthier, S.C., Doran, J.L., Banser, P.A., Kay, W.W., 1996. J. of Bacteriol. 178, 3, 662 - 667.
Contreras, J., Fernando, L., Alocilja, E., Salazar, F., Bacay, B., 2016. Int. J. Sci. Basic Appl. Res. IJSBAR 26, 138–157.
Dehdashtian, S., Gholivand, M.B., Shamsipur, M., Kariminia, S., 2016. Mater. Sci. Eng. C 58, 53–59.
Desrosier, J.P., Lara, J.C., 1981. J. Bacteriol. 145, 613–619.
Dewey-Mattia, D., Manikonda, K., Vieira, A., 2014. [WWW Document]. Cent. Dis. Control Prev. URL http://www.cdc.gov/foodsafety/pdfs/foodborne-outbreaks-annual-report-2014-508.pdf (accessed 5.23.16).
Diaz-Quiñonez, A., Martin-Orozco, N., Isibasi, A., Ortiz-Navarrete, V., 2004. Infect. Immun. 72, 3059–3062.
Disney, M.D., Seeberger, P.H., 2004. Chem. Biol. 11, 1701–1707.
Duan, N., Wu, S., Zhu, C., Ma, X., Wang, Z., Yu, Y., Jiang, Y., 2012. Anal. Chim. Acta 723, 1–6.
Duan, N., Xu, B., Wu, S., Wang, Z., 2016. Anal. Sci. 32, 431–436.
FDA, 2015. [WWW Document]. URL http://www.fda.gov/Food/FoodborneIllnessContaminants/FoodborneIllnessesNeedToKnow/ucm103263.htm (accessed 8.21.17).
Fernandes, A.M., Abdalhai, M.H., Ji, J., Xi, B.-W., Xie, J., Sun, J., Noeline, R., Lee, B.H., Sun, X., 2015. Biosens. Bioelectron. 63, 399–406.
Fernandes, J.C., Eaton, P., Gomes, A.M., Pintado, M.E., Xavier Malcata, F., 2009. Ultramicroscopy, Proceedings of the 10th International Scanning Probe Microscopy Conference 109, 854–860.
Firon, N., Ofek, I., Sharon, N., 1983. Carbohydr. Res. 120, 235–249.
Fratila, R.M., Moros, M., de la Fuente, J.M., 2016. Anal. Bioanal. Chem. 408, 1783–1803.
Galdiero, S., Falanga, A., Cantisani, M., Tarallo, R., Elena Della Pepa, M., D'Oriano, V., Galdiero, M., 2012. Microbe-host interactions: structure and role of Gram-negative bacterial porins. Curr. Protein Pept. Sci. 13, 843–854.
Galhoum, A., Mafhouz, M., Abdel-Rehem, S., Gomaa, N., Atia, A., Vincent, T., Guibal, E., 2015. Nanomaterials 5, 154–179.
Gayathri, C.H., Mayuri, P., Sankaran, K., Kumar, A.S., 2016. Biosens. Bioelectron. 82, 71–77.
Ge, Y., Zhang, Y., He, S., Nie, F., Teng, G., Gu, N., 2009. Nanoscale Res. Lett. 4, 287–295.
Gil-Cruz, C., Bobat, S., Marshall, J.L., Kingsley, R.A., Ross, E.A., Henderson, I.R., Leyton, D.L., Coughlan, R.E., Khan, M., Jensen, K.T., Buckley, C.D., Dougan, G., MacLennan, I.C.M., López-Macías, C.,

Cunningham, A.F., 2009. Proc. Natl. Acad. Sci. 106, 9803–9808. https://doi.org/10.1073/pnas.0812431106
Gohar, M., Faegri, K., Perchat, S., Ravnum, S., Okstad, O.A., Gominet, M., Kolsto, A.-B., Lereclus, D., 2008. The PlcR virulence regulon of Bacillus cereus. PLoS One 3, e2793.
Haseley, S.R., 2002. Anal. Chim. Acta 457, 39–45.
Havelaar, A.H., Kirk, M.D., Torgerson, P.R., Gibb, H.J., Hald, T., Lake, R.J., Praet, N., Bellinger, D.C., de Silva, N.R., Gargouri, N., Speybroeck, N., Cawthorne, A., Mathers, C., Stein, C., Angulo, F.J., Devleesschauwer, B., on behalf of World Health Organization Foodborne Disease Burden Epidemiology Reference Group, 2015. PLOS Med. 12, e1001923.
Helander, I.M., Nurmiaho-Lassila, E.-L., Ahvenainen, R., Rhoades, J., Roller, S., 2001. Int. J. Food Microbiol. 71, 235–244.
Horák, D., Babic, M., Jendelová, P., Herynek, V., Trchová, M., Pientka, Z., Pollert, E., Hájek, M., Syková, E., 2007. Bioconjug. Chem. 18, 635–644.
Hormozi-Nezhad, M.R., Seyedhosseini, E., Robatjazi, H., 2012. Sci. Iran. 19, 958–963.
Huang, H., Ruan, C., Lin, J., Li, M., Cooney, L.M., Oliver, W.F., Li, Y., Wang, A., 2011. Trans. ASABE 54, 1015–1024.
Hwang, J., Kwon, D., Lee, S., Jeon, S., 2016. Rsc Adv. 6, 48445–48448.
Issa, B., Obaidat, I., Albiss, B., Haik, Y., 2013. Int. J. Mol. Sci. 14, 21266–21305.
Jain, S., Chen, J., 2007. J. Food Prot. 70, 2473–2479.
Jansaento, W., Jangpatarapongsa, K., Polpanich, D., Wonglumsom, W., 2016. Food Sci. Biotechnol. 25, 193–198.
Joo, J., Yim, C., Kwon, D., Lee, J., Shin, H.H., Cha, H.J., Jeon, S., 2012. The Analyst 137, 3609.
Joys, T.M., 1985. J. Biol. Chem. 260, 16758–16761.
Kanayeva, D.A., Wang, R., Rhoads, D., Erf, G.F., Slavik, M.F., Tung, S., Li, Y., 2012. J. Food Prot. 75, 1951–1959.
Kimura, M., Fukushima, H., Sagawa, Y., Setsu, K., Hara, H., Inoue, S., 2009. IEEE Trans. Electron Devices 56, 2114–2119.
Koebnik, R., Locher, K.P., Van Gelder, P., 2000. Mol. Microbiol. 37, 239–253.
Kong, M., Chen, X.G., Xing, K., Park, H.J., 2010. Int. J. Food Microbiol. 144, 51–63.
Korhonen, T.K., Lounatmaa, K., Ranta, H., Kuusi, N., 1980. J. Bacteriol. 144, 800–805.
Kuang, H., Cui, G., Chen, X., Yin, H., Yong, Q., Xu, L., Peng, C., Wang, L., Xu, C., 2013. Int. J. Mol. Sci. 14, 8603–8610.
Kukkonen, M., Saarela, S., Lähteenmäki, K., Hynönen, U., Westerlund-Wikström, B., Rhen, M., Korhonen, T.K., 1998. Infect. Immun. 66, 4965–4970.
Kulshin, V.A., Zahringer, U., Linkner, B., Jager, K.-E., Dmitriev, B.A., Rietschel, E.T., 1991. Eur. J. Biochem. 198, 697–704.
Leitgeb, M., Heržič, K., Podrepšek, G.H., Hojski, A., Crnjac, A., Knez, Ž., 2014. Acta Chim. Slov. 61.
Lepoitevin, M., Lemouel, M., Bechelany, M., Janot, J.-M., Balme, S., 2015. Microchim. Acta 182, 1223–1229.
Lesman-Movshovich, E., Gilboa-Garber, N., 2003. J. Dairy Sci. 86, 2276–2282.
Li, S., Liu, H., Deng, Y., Lin, L., He, N., 2013. J. Biomed. Nanotechnol. 9, 1254–1260.
Lim, D., Villame, R.G., Quiñones, G.J., Vera, D. de, Notorio, R., Fernando, L., Alocilja, E., 2017. Philipp. J. Pathol. 2, 47.
Lin, C.-C., Yeh, Y.-C., Yang, C.-Y., Chen, C.-L., Chen, G.-F., Chen, C.-C., Wu, Y.-C., 2002. J. Am. Chem. Soc. 124, 3508–3509.
Lin, H., Lu, Q., Ge, S., Cai, Q., Grimes, C.A., 2010. Sens. Actuators B Chem. 147, 343–349.
Lindhorst, Thisbe K., 2011. Rauter, A.P., Lindhorst, T. K. (Eds.), Carbohydrate Chemistry: Chemical and Biological Approaches, Vol 37. Royal Soc Chemistry, Cambridge, pp. 194–207.
Liu, G., Yang, X., Li, T., Yu, H., Du, X., She, Y., Wang, J., Wang, S., Jin, F., Jin, M., Shao, H., Zheng, L., Zhang, Y., Zhou, P., 2015. Microchim. Acta 182, 1983–1989.

Liu, H., Zhan, F., Liu, F., Zhu, M., Zhou, X., Xing, D., 2014. Biosens. Bioelectron. 62, 38–46.
Liu, X., Hu, Y., Zheng, S., Liu, Y., He, Z., Luo, F., 2016. Sens. Actuators B Chem. 230, 191–198.
Lu, A.-H., Salabas, E.L., Schüth, F., 2007. Angew. Chem. Int. Ed. 46, 1222–1244.
Luo, Y., Nartker, S., Wiederoder, M., Miller, H., Hochhalter, D., Drzal, L.T., Alocilja, E.C., 2012. IEEE Trans. Nanotechnol. 11, 676–681.
Mahdavi, M., Ahmad, M., Haron, M., Namvar, F., Nadi, B., Rahman, M., Amin, J., 2013. Molecules 18, 7533–7548.
Malhotra, S., Welling, M.N., Mantri, S.B., Desai, K., 2016. J. Biomed. Mater. Res. B Appl. Biomater. 104, 993–1003.
Malic, L., Zhang, X., Brassard, D., Clime, L., Daoud, J., Luebbert, C., Barrere, V., Boutin, A., Bidawid, S., Farber, J., Corneau, N., Veres, T., 2015. Lab Chip 15, 3994–4007.
Manni, L., Ghorbel-Bellaaj, O., Jellouli, K., Younes, I., Nasri, M., 2010. Appl. Biochem. Biotechnol. 162, 345–357.
Matta, L.L., Karuppuswami, S., Chahal, P., Alocilja, E.C., 2018. Biosens. Bioelectron. 12.
McDonough, 1965. J Mol Biol 12, 342–355.
Mellegard, H., From, C., Christensen, B.E., Granum, P.E., 2011. Int. J. Food Microbiol. 149, 218–225.
Meng, X., Li, Fulai, Li, Fan, Xiong, Y., Xu, H., 2017. Sens. Actuators B Chem. 247, 546–555.
Mukherjee, M., De, S., 2017. Mater. Sci. Eng. C 75, 133–148.
Muller, A., Thomas, G.H., Horler, R., Brannigan, J.A., Blagova, E., Levdikov, V.M., Fogg, M.J., Wilson, K.S., Wilkinson, A.J., 2005. Mol. Microbiol. 57, 143–155.
Mun, S., Choi, S.-J., 2015. Biochip J. 9, 10–15.
Muñoz, A., Sigwalt, D., Illescas, B.M., Luczkowiak, J., Rodríguez-Pérez, L., Nierengarten, I., Holler, M., Remy, J.-S., Buffet, K., Vincent, S.P., Rojo, J., Delgado, R., Nierengarten, J.-F., Martín, N., 2016. Nat. Chem. 8, 50–57.
Neeser, J.-R., Koellreutter, B., Wuersch, P., 1986. Infect. Immun. 52, 428–436.
Nikaido, H., 2003. Microbiol. Mol. Biol. Rev. MMBR 67, 593–656.
Obaidat, I., Issa, B., Haik, Y., 2015. Nanomaterials 5, 63–89. https://doi.org/10.3390/nano5010063
Oxaran, V., Ledue-Clier, F., Dieye, Y., Herry, J.-M., P?choux, C., Meylheuc, T., Briandet, R., Juillard, V., Piard, J.-C., 2012. PLoS ONE 7, e50989.
Pal, S., Alocilja, E.C., 2010. Biosens. Bioelectron. 26, 1624–1630.
Park, J.Y., Jeong, H.Y., Kim, M.I., Park, T.J., 2015. J. Nanomater. Aricle ID 527126.
Park, S., Kim, G.-H., Park, S.-H., Pai, J., Rathwell, D., Park, J.-Y., Kang, Y.-S., Shin, I., 2015. J. Am. Chem. Soc. 137, 5961–5968.
Piette, J.P., Idziak, E.S., 1991. Appl. Environ. Microbiol. 57, 1635–1639.
Pokorná, M., Cioci, G., Perret, S., Rebuffet, E., Kostlánová, N., Adam, J., Gilboa-Garber, N., Mitchell, E.P., Imberty, A., Wimmerová, M., 2006. Biochemistry (Mosc.) 45, 7501–7510.
Prasad, N.K., Panda, D., Singh, S., Mukadam, M.D., Yusuf, S.M., Bahadur, D., 2005. J. Appl. Phys. 97, 10Q903.
Pratt, L.A., Kolter, R., 1998. Mol. Microbiol. 30, 285–293.
Raj, V., Vijayan, A.N., Joseph, K., 2015. Sens. Bio-Sens. Res. 5, 33–36.
Ramalingam, K., 2005. Biochem. Cell. Arch. 5, 137–143.
Safina, G., Vanlier, M., Danielsson, B., 2008. Talanta 77, 468–472.
Sanchez-Ramirez, J., Martinez-Hernandez, J.L., Segura-Ceniceros, P., Lopez, G., Saade, H., Medina-Morales, M.A., Ramos-Gonzalez, R., Aguilar, C.N., Ilyina, A., 2017. Bioprocess Biosyst. Eng. 40, 9–22.
Sattarahmady, N., Tondro, G.H., Gholchin, M., Heli, H., 2015. Biochem. Eng. J. 97, 1–7.
Setterington, E.B., Alocilja, E.C., 2012. Biosensors 2, 15–31.
Sharon, N., Eshdat, Y., Silverblatt, F.J., Ofek, I., 1981. Ciba Found. Symp. 80, 119–141.
Shi, S., Jia, J., Guo, X., Zhao, Y., Chen, D., Guo, Y., Zhang, X., 2016. Int. J. Nanomedicine Volume 11, 6499–6506.

Shi, X.-Z., Yu, X.-Q., 2012. Amino Acids 42, 2383–2391.
Shim, W.-B., Lee, C.-W., Kim, M.-G., Chung, D.-H., 2014a. Anal. Methods 6, 9129–9135.
Shim, W.-B., Song, J.-E., Mun, H., Chung, D.-H., Kim, M.-G., 2014b. Anal. Bioanal. Chem. 406, 859–866.
Shuguang Wang, Lawson, R., Ray, P.C., Hongtao Yu, 2011. Toxicol. Ind. Health 27, 547–554.
Singh, S.P., Singh, S.R., Williams, Y.U., Jones, L., Abdullah, T., 1995. Infect. Immun. 63, 4600–4605.
Sinha, N., Mohan, S., Lipschultz, C.A., Smith-Gill, S.J., 2002. Biophys. J. 83, 2946–2968.
Soares, P.I.P., Machado, D., Laia, C., Pereira, L.C.J., Coutinho, J.T., Ferreira, I.M.M., Novo, C.M.M., Borges, J.P., 2016. Carbohydr. Polym. 149, 382–390.
Sommer, R., Hauck, D., Varrot, A., Wagner, S., Audfray, A., Prestel, A., Möller, H.M., Imberty, A., Titz, A., 2015. ChemistryOpen 4, 756–767.
Stahlhut, S.G., Tchesnokova, V., Struve, C., Weissman, S.J., Chattopadhyay, S., Yakovenko, O., Aprikian, P., Sokurenko, E.V., Krogfelt, K.A., 2009. J. Bacteriol. 191, 6592–6601.
Sun, Q., Zhao, G., Dou, W., 2016. Sens. Actuators B Chem. 226, 69–75.
Sung, Y.J., Suk, H.-J., Sung, H.Y., Li, T., Poo, H., Kim, M.-G., 2013. Biosens. Bioelectron. 43, 432–439.
Tran, S.L., Guillemet, E., Gohar, M., Lereclus, D., Ramarao, N., 2010. J. Bacteriol. 192, 2638–2642.
Trungkathan, S., Polpanich, D., Smanmoo, S., Tangboriboonrat, P., 2J. Appl. Polym. Sci. 131, 40012.
Unni, M., Uhl, A.M., Savliwala, S., Savitzky, B.H., Dhavalikar, R., Garraud, N., Arnold, D.P., Kourkoutis, L.F., Andrew, J.S., Rinaldi, C., 2017. ACS Nano 11, 2284–2303.
Unsoy, G., Yalcin, S., Khodadust, R., Gunduz, G., Gunduz, U., 2012. J. Nanoparticle Res. 14, 1–13.
Uribe, E., Steele, T.J., Richards, R.C., Ewart, K.V., 2013. Biochim. Biophys. Acta BBA - Gen. Subj. 1830, 2129–2138.
Verma, M.S., Rogowski, J.L., Jones, L., Gu, F.X., 2015. Biotechnol. Adv. 33, 666–680.
Vetrone, S.A., Huarng, M.C., Alocilja, E.C., 2012. Sensors 12, 10487–10499.
Waalen, K., Sletten, K., Fro'holm, L.O., Vaisanen, V., Korhonen, T.K., 1983. FEMS Microbiol. Lett. 16, 149–151.
Wan, Y., Sun, Y., Qi, P., Wang, P., Zhang, D., 2014. Biosens. Bioelectron. 55, 289–293.
Wang, D., Chen, Q., Huo, H., Bai, S., Cai, G., Lai, W., Lin, J., 2017. Food Control 73, 555–561.
Wang, J., Chen, Z., Li, Z., Yang, Y., 2016. Food Chem. 204, 135–140.
Wang, X., Huang, Y., Wu, S., Duan, N., Xu, B., Wang, Z., 2016. Int. J. Food Microbiol. 237, 172–179.
Wang, Y., Alocilja, E.C., 2015. J. Biol. Eng. 9, 16, 1-7.
Wang, Y., Fewins, P.A., Alocilja, E.C., 2015. IEEE Sens. J. 15, 4692–4699.
Wang, Y., Ye, Z., Si, C., Ying, Y., 2013. Food Chem. 136, 1303–1308.
Webster, M.S., Cooper, J.S., Chow, E., Hubble, L.J., Sosa-Pintos, A., Wieczorek, L., Raguse, B., 2015. Sens. Actuators B-Chem. 220, 895–902.
WHO, 2015. [WWW Document]. URL http://www.who.int/foodsafety/areas_work/foodborne-diseases/ferg/en/
Xayarath, B., Marquis, H., Port, G.C., Freitag, N.E., 2009. Mol. Microbiol. 74, 956–973.
Xu, H., Murdaugh, A.E., Chen, W., Aidala, K.E., Ferguson, M.A., Spain, E.M., Núñez, M.E., 2013. Langmuir 29, 3000–3011.
Yazgan, I., Noah, N.M., Toure, O., Zhang, S., Sadik, O.A., 2014. Biosens. Bioelectron. 61, 266–273.
Zhang, W., Hu, Q., Su, Y., Zheng, X., 2014. J. Electroanal. Chem. 719, 72–76.
Zhao, Y., Li, Y., Jiang, K., Wang, J., White, W.L., Yang, S., Lu, J., 2017. Food Control 71, 110–116.
Zhiyang, L., Lei, H., Nongyue, H., Zhiyang, S., Hua, W., Song, L., Hongna, L., Yabin, D., 2010. Acta Chim. Sin. 68, 251–256.

Highlights

- state-of-the-art nano-biosensing methods designed for rapid bacterial extraction using suspended magnetic nanoparticles (MNP)
- attention is also paid to those methods that report success in more complex matrices
- applications that use electrically active nanoparticles (EANP) to intensify their optical detection or make use of electrochemical methods
- carbohydrate ligand binding selectivity from a broad spectrum of research areas
- a novel rapid (30 min) MNP-cell-AuNP (gold nanoparticle) nano-biosensing method is introduced